

INFRARED SUPERNOVA REMNANTS IN THE LARGE MAGELLANIC CLOUD

J. SEOK

Department of Physics and Astronomy, Seoul National University, Seoul 151-747, Korea

E-mail: jyseok@astro.snu.ac.kr

(Received July 01, 2012; Accepted July 26, 2012)

ABSTRACT

We present preliminary results of supernova remnants (SNRs) in the Large Magellanic Cloud (LMC) seen by AKARI as well as Spitzer. By examining the AKARI LMC survey and the Spitzer data, we have searched for IR counterparts to 45 known SNRs in the LMC and could identify 28 SNRs with associated IR emission. 13 SNRs among them are newly detected in IR bands. For the entire IR SNRs, we make a catalog containing general information and the AKARI and/or Spitzer fluxes. Using the catalog, their IR colors and the possible correlation of the IR fluxes with the X-ray fluxes are examined. For some interesting SNRs, we have performed NIR spectroscopy with AKARI. An aromatic feature at $3.3 \mu\text{m}$ can be identified in LMC SNR N49. We investigate the characteristics of the IR features and discuss the PAH emission mechanism in SNRs.

Key words: ISM: dust, extinction; infrared: ISM: lines and bands; ISM: supernova remnants; Magellanic Clouds

1. INTRODUCTION

The Large Magellanic Cloud (LMC) has several advantages for studying supernova remnants (SNRs). Detailed structures of SNRs can be examined due to its proximity (~ 50 kpc), and there are more than forty radio/X-ray SNRs offering non-biased samples. The most important advantage, especially in terms of studying IR emission, is that the LMC is located far off from the Galactic plane, so we can avoid much back/foreground confusion by a number of IR sources.

Since the IRAS was launched, several IR studies on Galactic SNRs have been done by using large number of sources. There are statistical studies of entire Galactic SNRs (e.g., Arendt, 1989; Saken et al., 1992); Arendt (1989) found 51 SNRs with probable/possible IR emission out of 157 Galactic SNRs and probed the presence of correlations between IR and other wavelength fluxes. The above studies, however, had instrumental limitations in both spatial resolution and sensitivity, and more seriously, confusion with other Galactic sources such as HII regions was a big problem.

For LMC SNRs, there are some previous works using IRAS data, but the early works could not detect many IR SNRs because of their relatively small sizes compared to the spatial resolution and the lack of known SNR samples at those times. Recently, most of the LMC was observed by the Spitzer SAGE survey ($7^\circ \times 7^\circ$, Meixner et al., 2006), and AKARI has performed a large scale survey of the LMC (Ita et al., 2008). The AKARI telescope has continuous coverage of imaging from $2.5 - 26 \mu\text{m}$, in particular, the 11 and $15 \mu\text{m}$ bands are unique. While there are various studies about individual SNRs using the numerous IR data, more statistical studies including the total SNRs in the LMC have not been done yet, so it becomes essential to study SNRs and their environment with large number of sources.

2. STATISTICAL STUDIES OF LMC SNRS

2.1. SNR Identification and IR Properties

To search for IR emission from SNRs in the LMC, we use the AKARI LMC survey (Ita et al., 2008) as well

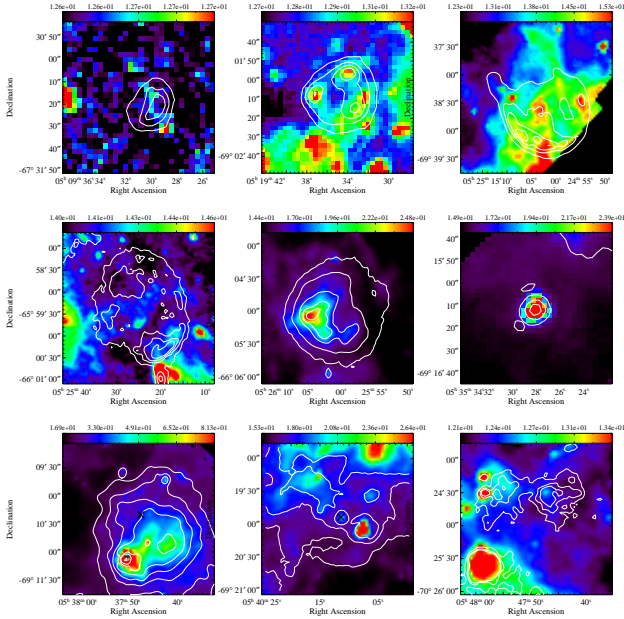


Fig. 1. AKARI S11 band images of nine SNRs. *Top*: 0509–67.5, 0519–69.0, and N132D. *Middle*: N49B, N49, and SN 1987A. *Bottom*: N157B, N158A, and 0548–70.4. Contours show the brightness distribution of each SNR in the L24 band. “x” marks represent the positions of pulsars in N157B and N158A. The units on the colorbar of the AKARI images are MJy sr⁻¹.

as the Spitzer archival data. 21 SNRs are included in the AKARI LMC survey (~ 10 deg²), and Spitzer data are available for all the known SNRs. To confirm IR emission associated with SNRs, we compare the IR data with other multi-wavelength data such as radio (Dickel et al., 2005), optical (Smith et al., 2000), and Chandra X-ray images. Finally, we could identify 28 out of 45 SNRs in the whole LMC (nine SNRs in the AKARI survey) which show associated IR emission in the AKARI and/or Spitzer bands. Among them, IR morphologies of 13 SNRs are identified in this work for the first time.

We measure the AKARI and Spitzer fluxes for the SNRs and list them in preliminary catalogs. All 28 SNRs are detected in the 24 μ m bands, and half of them are also seen at shorter wavelengths. Many of SNRs show shell-like structures, but some also show complex morphologies consisting of filamentary and/or knotty structures. The nine SNRs detected in the AKARI bands are shown in Figure 1. Although all SNRs are seen in the 24 μ m band (contours), some SNRs such as

SNR 0519–69.0, N49, and SN 1987A show clear emission in the 11 μ m band. Other SNRs are confused by background emission and/or do not show distinguishable emission.

For the SNRs detected in the Spitzer IRAC bands, we compare their IRAC colors ($F_{3.6}/F_{5.8}$ and $F_{4.5}/F_8$). It is known that the origin of IR emission can be inferred by the IRAC colors (Reach et al., 2006). Adopting presumable IRAC colors associated with ionic/molecular shocks, polycyclic aromatic hydrocarbons (PAHs), and synchrotron emission from Reach et al., it is found that most LMC SNRs fall on the area of the diagram for SNRs associated with molecular shocks. Some other SNRs fall on the area for SNRs with PAH emission, and only few have IRAC colors of SNRs associated with ionic shocks. However, it is noticeable that N49 and N63A, previously thought to be ionic-line dominated (e.g., Williams et al., 2006), actually have IRAC colors for molecular shocks. This could indicate that one should be cautious to infer the IR origin using the IRAC colors.

2.2. Comparison between IR and X-ray

We compare the AKARI and Spitzer 24 μ m fluxes (νF_ν) to Chandra soft band (0.3–2 keV) X-ray fluxes. As expected from morphological similarities between the 24 μ m and X-ray images, the 24 μ m fluxes are well-correlated with the X-ray fluxes. In fact, this good correlation is expected because the MIR emission in a SNR is indeed physically related to X-ray emission. Dust continuum is considered as the primary origin of MIR emission (> 10 μ m) from a SNR, which is known to arise from collisional heating by hot plasma emitting X-ray emission. Dust temperature directly depends on the plasma properties, in particular, electron density and electron temperature (e.g., Dwek, 1987), which can result in the tight correlation between IR and X-ray emission.

3. PAH EMISSION FROM A SNR

PAH emission is thought to be one of the emission mechanisms for IR emission from SNRs (e.g., Reach et al., 2006). In PAH processing, interstellar shocks are known to play a crucial role. It is thought that PAHs could be the fragmentation of dust grains through shattering collision in fast interstellar shocks (e.g., Jones et al., 1996). Also, interstellar shock waves are one of the main mechanisms to destroy PAH molecules. In

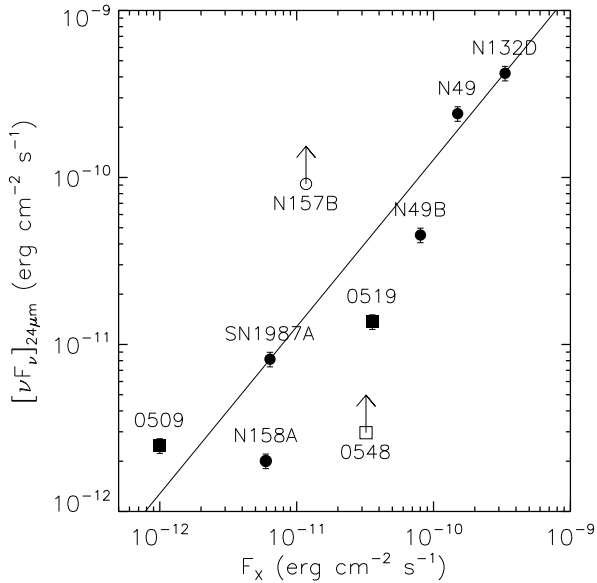


Fig. 2. AKARI 24 μm versus Chandra X-ray (0.3 – 2 keV) fluxes. Square symbols are for Type Ia SNRs and circles for Type II SNRs. Open symbols are for the objects of which fluxes are extracted from limited areas. In the case of N158A, the fluxes are extracted only from its PWN. Note that the symbol of N158A is filled here since both the IR and X-ray fluxes are extracted from its PWN. The solid line represents best-fit linear-regression line.

spite of plentiful observations of PAH features, however, there are still unanswered questions on the role of interstellar shocks in the evolution of PAHs. Particularly, how SN shocks affect PAH molecules is barely explored. Detection of PAH features in SNRs is unexpectedly rare, recalling that the one of their formation process is related to interstellar shocks.

3.1. Detection of 3.3 μm Aromatic Feature in N49

Since PAH molecules in shock regions are supposed to be able to survive only in those with dense clumps (Micelotta et al., 2010), SNRs interacting with dense circumstellar or interstellar material would be good candidates for detecting PAH emission. We have targeted an IR-bright SNR, N49 with AKARI, which is one of the SNRs interacting with ambient molecular clouds in the LMC. We performed NIR (2.5 – 5 μm) spectroscopy toward N49 using AKARI. As a result, we could extract final spectra from five different regions with a background spectrum as shown in Figure 2. Hydrogen recombination lines and H_2 molecular lines are

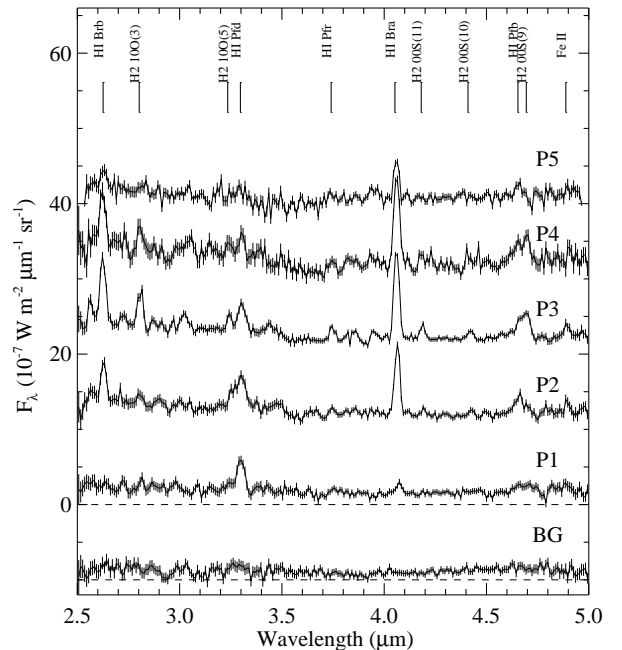


Fig. 3. AKARI NIR spectra of N49 (Seok et al., 2012). For convenience, the spectra are shifted by 1, 2, 3, and 4 $\times 10^{-6} \text{ W m}^{-2} \mu\text{m}^{-1} \text{ sr}^{-1}$ for P2 to P5, respectively. Background spectrum is shown in the bottom (shifted by $-1 \times 10^{-6} \text{ W m}^{-2} \mu\text{m}^{-1} \text{ sr}^{-1}$). Noticeable lines are labeled at their vacuum wavelengths.

detected in the several spectra, and the 3.3 μm aromatic feature can be identified from a SNR for the first time (see more in Seok et al., 2012).

Using all the spectra covering the PAH-bright area of N49 in the east, we can construct line maps of H_2 , PAH, and $\text{Br}\alpha$ emissions. The morphology of PAH emission seemingly is associated with those of emission at other wavelengths. The peak of PAH emission is found to be located at the tip of the bright wedge-shaped emission region, and the overall shape also shows enhanced emission along the wedge-shaped region. This strongly supports that the PAH emission is indeed related to the SNR.

3.2. PAH Emission Mechanism

We propose a model of the PAH emitting condition in N49. As a shock is retarded by a dense gas, the temperature of the postshock gas can substantially decrease. The PAH lifetime under these circumstances can significantly increase. PAHs in the central region (or un-

shocked region) of the molecular clumps (and the dense filaments) can be heated by UV photons that mainly originate in the radiative shell. In the case of the PAH emission observed outside the shock front, it is most likely that the preexisting PAH molecules are heated by the radiative precursors and produce the emission features. In summary, PAH emission can be associated with shocked ionic gas or molecular gas when the shock is sufficiently retarded combined with the existence of a heating source such as UV photons.

4. CONCLUSION

The LMC is eminently suitable to study IR emission from SNRs due to its proximity as well as less IR confusion. We carry out statistical studies of IR SNRs in the LMC and a detailed study of PAH emission in the SNR N49 using two advanced IR space telescopes, the AKARI and Spitzer. AKARI and Spitzer survey observations of the LMC enable us to identify 28 IR SNRs out of 45 known SNRs, and 13 SNRs among 28 are found for the first time by this work. We investigate the origin of IR emission from the SNRs based on their Spitzer IRAC colors, but one should be cautious to conclude the IR origin by using only these colors. Good correlation between IR and X-ray emission is found, which reflects their physical relation between the two emission mechanisms. PAH emission is thought to be one of the dominant sources for the IR emission from SNRs. AKARI NIR spectroscopic observations reveal the presence of $3.3\ \mu\text{m}$ aromatic features in N49, which can give important information on the PAH processing by interstellar shocks. The PAH emission shows spatial correlation with shocked ionic/molecular gas, and would be produced in dense medium where SN shocks are sufficiently retarded with abundant UV photons.

ACKNOWLEDGEMENTS

The AKARI conference is hosted by Seoul National University with support from many other institutes. We thank all the organizers of the conference. This research was supported by Basic Science Research Program through the National Research Foundation of Korea (NRF) funded by the Ministry of Education, Science and Technology (NRF-2011-0007223).

REFERENCES

- Arendt, R. G., 1989, An Infrared Survey of Galactic Supernova Remnants, *ApJS*, 70, 181
- Dickel, J., McIntyre, V., Gruendl, R., & Milne, D., 2005, A 4.8 and 8.6 GHz Survey of the Large Magellanic Cloud. I. The Images, *AJ*, 129, 790
- Dwek, E., 1987, The Infrared Diagnostic of a Dusty Plasma with Applications to Supernova Remnants, *ApJ*, 322, 812
- Ita, Y., et al., 2008., AKARI IRC Survey of the Large Magellanic Cloud: Outline of the Survey and Initial Results, *PASJ*, 60, 435
- Jones, A. P., et al., 1996, Grain Shattering in Shocks: The Interstellar Grain Size Distribution, *ApJ*, 469, 740
- Meixner, M., et al., 2006, Spitzer Survey of the Large Magellanic Cloud: Surveying the Agents of a Galaxy's Evolution (SAGE). I. Overview and Initial Results, *AJ*, 132, 2268
- Micelotta, P., et al., 2010, Polycyclic Aromatic Hydrocarbon Processing in a Hot Gas, *A&A*, 510, A37
- Reach, W. T., et al., 2006, A Spitzer Space Telescope Infrared Survey of Supernova Remnants in the Inner Galaxy, *AJ*, 131, 1479
- Saken, J. M., Fesen, R. A., & Shull, J. M., 1992, An IRAS Survey of Galactic Supernova Remnants, *ApJS*, 81, 715
- Seok, J. Y., Koo, B.-C., & Onaka, T., 2012, Detection of the $3.3\ \mu\text{m}$ Aromatic Feature in the Supernova Remnant N49 with AKARI, *ApJ*, 744, 160
- Smith, C., Leiton, R., & Pizarro, S., 2000, The UM/CTIO Magellanic Cloud Emission Line Survey (MCELS), *ASPC*, 221, 83
- Williams, R. M., Chu, Y.-H., & Gruendl, R., 2006, Supernova Remnants in the Magellanic Clouds. VII. Infrared Emission from Supernova Remnants, *AJ*, 132, 1877